Development of a flow loop system for scale management study in geothermal systems: From a static to a dynamic study

Yunqi Wang, Arjen Boersma, Francesco Pizzocolo, Frank Vercauteren, Hartmut Fischer

High Tech Campus 25, 5656 AE, Eindhoven, the Netherlands

yunqi.wang@tno.nl

Keywords: Scaling, deposition, Monitoring, Geothermal well, pipeline, static, dynamic flow loop

ABSTRACT

The formation of solid deposition in geothermal systems presents a significant constraint in the design, operation and profitability of geothermal power plants. Scale forms under supersaturation conditions, wherever the mixing of water from different feed zones takes place or in case of sudden pressure or temperature changes. To improve the efficiency of geothermal production, solid deposition should be prevented and/or controlled. In previous study (Boersma 2018), the influence of surface energy, surface roughness, and stiffness of the substrate on scale formation have been assessed by monitoring the scale deposition on a series of coatings on various steel plates in a static condition. In order to investigate all the aspects related to scale formation dynamically and to reach a full understanding of the scale deposition process, an experimental set-up has been designed and built to study deposition in a flow loop system.

1. INTRODUCTION

The formation of sparingly soluble inorganic salts known as 'scaling', is recognized as a major operational problem not only during oil and gas production, but also commonly during geothermal energy production. Scale causes equipment damage, contributes to corrosion and flow restriction, thus reducing the profitability and limiting the growth of geothermal energy in the market of renewable energies.

Calcium carbonate ($CaCO_3$) is one of the most insoluble scale type occurring in the production well and surface facilities, such as downhole tubing and pipelines, causing undesirable severe flow restriction. The formation of $CaCO_3$ scale deposition is mainly influenced by partial pressure of CO_2, temperature, pH, and scaling ions (Chen et al 2016). When the partial pressure of CO_2 drops near the wellbore, CO_2 starts to degas from the aqueous solution and result in pH increase. Subsequently, the driving force leads to the precipitation of $CaCO_3$. High temperature is another driving force causing $CaCO_3$ deposition due to faster kinetics. Meanwhile, as the solubility of $CaCO_3$ decreases as the temperature increases, $CaCO_3$ tends to crystallize at high temperature. Scaling salt ions can affect the thermal dynamics of the $CaCO_3$ formation. Higher concentration of scaling ions will result in higher superstation of scaling solution, which happens when two incompatible waters meet downhole (e.g. seawater and formation water). As a result, the mixed water become oversaturated with scale components and forms insoluble salts (Mavredaki 2014).

Most researches on scaling have been focused on the bulk phase or on seeded crystals (Nancollas et al 1971; Kazmleczak et al 1982) other than the growth of scaling directly on the surfaces. It has been recently revealed that the dominant growth kinetics of $CaCO_3$ in the bulk phase and on a surface is different (Zhang et al 2012). The scaling tendency on the casing inner surface depends on the water composition, the surface chemistry and morphology on the casing. In general, scale formation happens following the process of nucleation, precipitation and crystal growth. Only when the nucleus forms on the pipe surface, or forms in the liquid but adhere onto the surface, scale deposition can occur. In order to mitigate the scale deposition issues, the stages of surface nucleation and precipitation adherence to the surface should be prevented, which can be influenced by the surface properties of the pipe.

In our previous study, the parameters of surface energy, surface morphology, and bulk modulus of substrate material for $CaCO_3$ scale formation were studied in static tests (Boersma 2018). In order to monitor and understand the root cause of scaling kinetics under dynamic conditions that is more representative for down hole, a flow loop system capable of studying scale formation inside a tube or on a flat surface has been developed.

2. STATIC STUDY

2.1 Substrates and pre-treatment

Three steel substrates: labelled as QD, R and S (Q-lab Corporation) and one glass fibre reinforced (GFR) epoxy substrate were used. The roughness of the substrates was measured by Sensofar Optical Imaging Profiler, as shown in Table 1.

To change surface energy of substrates, the substrates were partially pre-treated by a range of different surface modifiers in types of fluorinated compounds, epoxy, polydimethylsiloxane (PDMS), silicate, and alkyl. The

Table 1: Surface roughness of substrates.

Substrate	Roughness, S_a (μm)	Peak area ratio, r_1	Area increase due to roughness, r_2
QD	0.38	0.81	1.01
R	1.18	0.49	1.05
S	1.02	0.78	1.27
GFR	0.044	0.93	1.01

Table 2: Surface energy for pre-treated and non-treated substrates

Substrate	**Surface modifier**		**γ_{total} [mN/m]**	**$\gamma_{dispersive}$ [mN/m]**	**γ_{polar} [mN/m]**
	Type	Name			
QD steel	Fluorinated	Fluoroacrylate	8.9 ± 0.66	8.5 ± 0.58	0.4 ± 0.08
		Fluorolink F10	14.1 ± 2.2	10.6 ± 1.48	3.5 ± 0.72
	Epoxy	Araldite (2:1)	32.2 ± 2.26	29.3 ± 0.68	2.8 ± 1.58
		Araldite (2.5:1)	29.4 ± 1.49	25.1 ± 0.74	4.2 ± 0.74
		Araldite (2:1.5)	34.6 ± 8.28	29.7 ± 6.43	4.9 ± 1.85
	PDMS	Sylgard 184	23 ± 0.78	22.1 ± 0.66	0.8 ± 0.12
	SiO_2	TEOS	29.7 ± 1.34	27.7 ± 0.86	2 ± 0.48
		SmartCoat	5.3 ± 0.38	5.2 ± 0.3	0.1 ± 0.08
	Alkyl	TEOS/DTMS (1:1)	21.1 ± 1.86	20 ± 1.58	1 ± 0.28
QD steel	N/A		36.7 ± 1.7	29.9 ± 1.0	6.8 ± 0.7
R steel	N/A		37.7 ± 1.3	30.6 ± 0.8	7.1 ± 0.6
S steel	N/A		32.7 ± 1.4	28.4 ± 1.1	4.4 ± 0.3
GFR epoxy	N/A		46.9 ± 4.0	38 ± 2.4	8.9 ± 1.7

modifiers were dissolved in solvent in a volume fraction of 2% and applied on the substrate using doctor blade and yield a 200 nm coating layer after heat treatment. The surface energies of the pre-treated and the non-treated substrates were measured by a surface tension machine (DSA100, Krüss), as listed in Table 2. The surface energy of modifiers were measured applied to the QD substrate because of small distortion from its low surface roughness.

2.2 Influence of substrate parameters on scale formation

The scale formation experiments were performed by gluing two plastic cylinders on the pre-treated area of one substrate. For experimental control, one cylinder was glued on the non-treated area. The scaling set-up is shown in Figure 1(a). All three cylinders were filled with 0.1 M $CaCl_2$ solution, and then the same volume of 0.2 M $NaHCO_3$ solution is added. The $CaCO_3$ gradually precipitated and formed on the substrate after an induction period. After 1 hour at room temperature, the cylinders were removed and the substrate was thoroughly washed to remove non-reacted chemicals. The scaling layer was then characterized after drying. The scale formation process were performed on all substrates.

The formed scale surface was characterized by spectrophotometer (USB4000, Ocean Optics), as shown in Figure 1(b). The reflected light intensities from the scale formed region I_{scale} and from the substrate region (without scale) $I_{sub.}$ were measured. The absorbance of the scaling layer, as an indication of amount of scale formed, was calculated as:

$$A = -\log(\frac{I_{scale}}{I_{sub}}) \qquad [1]$$

To access the scale that was grown on the surface, an adhesive tape was applied to remove the sedimented scale that was nucleated in the bulk solution. The force generated by adhesive tape was approximately 2.5 N/cm. When the scale was not firmly adherent to the substrate, it came off leaving behind a cleaner surface and resulted in a lower absorbance. The absorbance of scale layers formed on different surface were measured before and after application of adhesive tape, the absorbance difference (ΔA) and the absorbance after tape A_{scale} is shown in Figure 2 (modifiers of PDMS, Teos-DTMS and F10 were not performed on GFR epoxy substrate). As for the bare substrates, the lowest

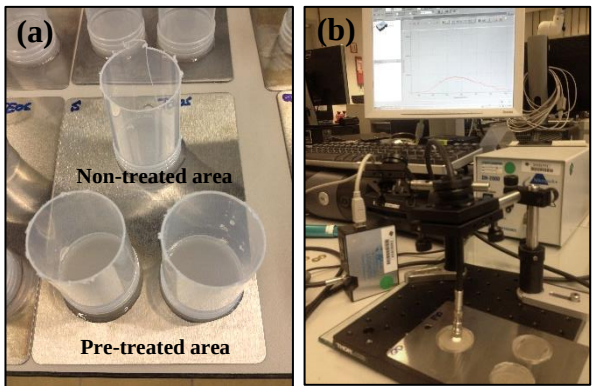

Figure 1: (a) Scale formation in plastic tubes on substrates. (b) Characterization of formed scale layer by light reflection method, images modified from (Boersma et al 2018).

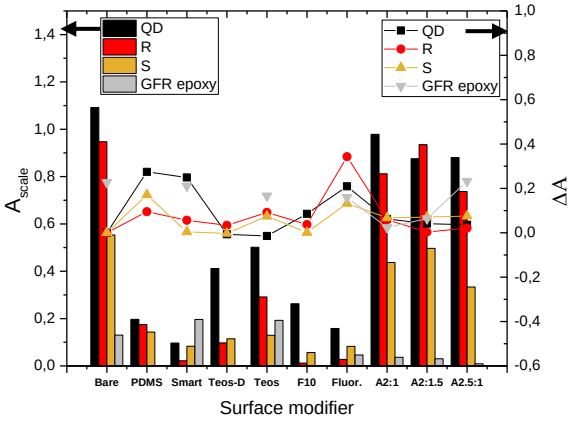

Figure 2: Light absorption of scale layer formed on different surface (left-axis), and light absorption difference before and after scale detachment by adhesive tape (right-axis).

amount of scale was formed on the GFR epoxy, and the highest was found on the QD steel panel disregarding the surface modifications. For PDMS, fluoracrylate and smartcoat per-treated surface, the scale came off relatively easy, as indicated of a larger ΔA value.

Work of adhesion which correlates the surface energy is an important parameter to determine scaling behaviour (van Krevelen, 1997).

$$W = \gamma_{13} + \gamma_{23} - \gamma_{12} \qquad [2]$$

where γ_{13}, γ_{23}, γ_{12} are interfacial energies between the phases of the scale [1], substrate [2] and water [3]. To reduce adhesion between the scale and the substrate, low interfacial energy γ_{12} is preferred, and hence large work of adhesion is favourable so that the substrate and scale prefer to be in contact with water. Furthermore, to include the effect of surface roughness, the work of adhesion can be modified to (Good 1998),

$$W = \gamma_{13} + \gamma_{23} r_2 - \gamma_{12} r_1 \qquad [3]$$

where r_1 and r_2 are the peak area ratio and the increased surface area due to roughness, respectively, referring to Table 1. r_1 is introduced because the scale is favourable to crystallize and in contact with the peak regions of the rough surface due to their high surface energy.

Research on the surface adhesion of biofouling shows that the surface elasticity is another parameter to consider (Chaudhury 2005). Kendall's model (Kendall 1971) describes the pull-off force (F) of a rigid cylinder stub with radius *a* from an elastic film with thickness *h*:

$$F = \pi a^2 \left(\frac{2WK}{h}\right)^{1/2} \qquad [4]$$

where *K* is the bulk modulus of the film. The bulk modulus of steel substrate is 160 GPa and 50 GPa for epoxy substrate. Because the modifier coating layer is very thin, its effects on surface bulk modulus is neglected. The relationship between the surface scaling tendency and the surface energy, surface roughness, and surface bulk modulus becomes:

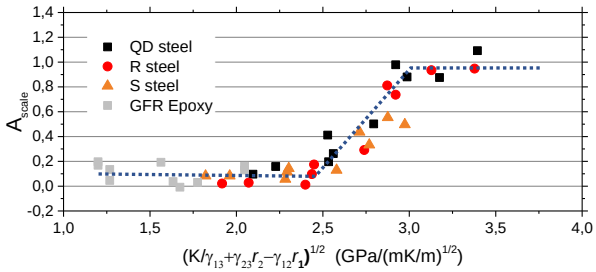

Figure 3: Correlation between scaling tendency and surface properties.

$$A_{scale} \sim \frac{F}{W} \sim \left(\frac{K}{W}\right)^{\frac{1}{2}} \sim \left(\frac{K}{\gamma_{13}+\gamma_{23}r_2-\gamma_{12}r_1}\right)^{\frac{1}{2}} \qquad [5]$$

The comparison of the scale tendency on all surface samples is shown in Figure 3. The value of $(K/\gamma_{13} + \gamma_{23}r_2 - \gamma_{12}r_1)^{1/2}$ can be used to indicate the surface scaling tendency. According to Figure 3, there is a transition region between low and high amount of scale formation, scale starts to develop when $(K/\gamma_{13} + \gamma_{23}r_2 - \gamma_{12}r_1)^{1/2}$ is higher than 2.5 $(GPa/(mN/m))^{1/2}$ until the value reaches 3 $(GPa/(mN/m))^{1/2}$ when the surface is fully covered with a scale layer.

The surface scale deposition behaviours were accessed on various coated steel and glass fibre reinforced epoxy substrates under static experimental conditions. In the next section, an experimental setup to study the scale deposit-forming processes under dynamic conditions is introduced.

3. DEVELOPMENT OF A DYNAMIC FLOW LOOP SYSTEM

In order to further investigate the effects of, e.g., flow phenomena, temperature gradient, pressure difference, etc., on the scale formation, a set-up capable of monitoring the scaling process under dynamic condition is developed. The set-up is composed of a circulation system where the scaling solution is kept in a temperature controlled reservoir and recycled though a flow loop. The test section of the loop consists of a tube which is surrounded by cooling fluid circulating in a jacket, as shown in Figure 4. The tube can be easily

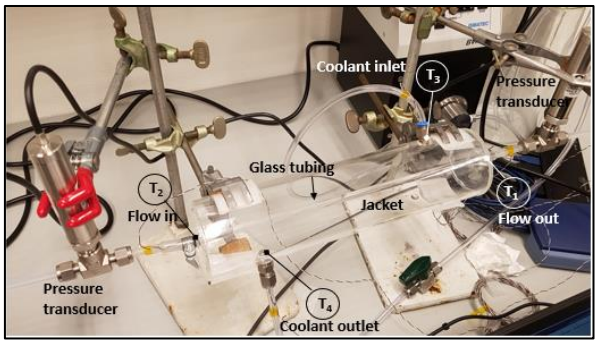

Figure 4: Test section of the flow loop to monitor deposition in tube. The circled *T* symbols indicate the positions of thermocouples placed. They are used to measure temperature profiles of solution flow and coolant.

changed to serve different deposition surface purpose. The deposition thickness in the tube during flow is monitored by heat transfer method (Chen 1997, Cordoba 2001) and pressure drop method (Chen 1997, Wang 2018).

To evaluate the effectiveness of this methodology, preliminary tests were performed by measuring the thickness of wax deposition by heat transfer method. Before the occurrence of deposition layer on the tube inner wall, the total resistance to heat transfer from the flowing fluid to the environment includes the resistance of convective heat transfer from the flowing fluid to the tube, heat conduction through the tube wall, and the heat transfer process from the tube to the environment. Once deposition is formed on the inner tube wall, it behaves as a thermal insulation. The added thermal resistance to the heat transfer from the flowing fluid to the coolant is proportional to the thickness of the deposition layer on the tube wall. The deposition thickness can be calculated from the recorded solution and coolant temperature profiles following the equation (Chen 1997):

$$\frac{T_f - T_e}{q_0} = \frac{1}{h_{dep}} \frac{r_o}{r_i - \delta_{dep}} + \frac{r_o}{k_{dep}} ln \frac{r_i}{r_i - \delta_{dep}} + \frac{r_o}{k_{tub}} ln \frac{r_o}{r_i} + \frac{1}{h_0} \quad [6]$$

where T_f and T_e are the flowing fluid temperature and the environment (coolant in the jacket) temperature, respectively; r_o and r_i are the outside and inside diameters of the tube, respectively, and δ_{dep} is the thickness of the deposition layer; h_0 is the heat transfer coefficient from the outside tube wall to the environment, which can be calculated using model for forced convection around a submerged object; h_{dep} is the heat transfer coefficient form the flowing fluid to the deposition layer, which can be determined by experimental method; k_{tub} and k_{dep} are the thermal conductivities of the tube and the deposition layer, respectively; q_0 is the heat flux through the tube wall, which can be obtained from the heat balance between the heat lost from the fluid and the heat transferred to the environment:

$$C_p \rho Q \Delta T_f = 2\pi r_O L q_0 \quad [7]$$

where C_p is the specific heat of the solution; ρ is the solution density; Q is the volumetric flow rate, ΔT_f is the fluid temperature drop over the deposition section, and L is the tube length. A set of experiments was performed at a hydrocarbon flowing solution of 30 °C and cooling water of 4 °C, and terminated at different times. The deposits that adhered to the tube wall were removed after each run, and then the tube was thoroughly rinsed. The wax deposition thickness calculated using the heat transfer method with time is shown in Figure 5. In the first run, the deposition of wax showed a steady increase with time up to 20 min and then reached a final fluctuating value. The wax deposited faster in the second run. For the following runs (3rd to 5th), the wax deposition on the tube wall

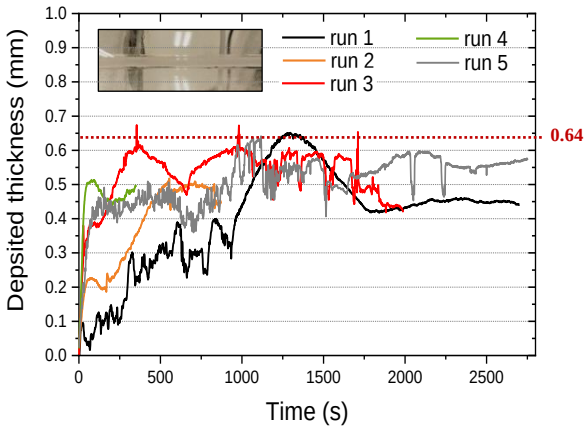

Figure 5: Measurement of deposited wax thickness in the tube for five runs with a circulating flow loop system with the heat transfer method. The inset shows the photo of deposited tube.

Table 3: Comparison of the heat transfer method and direct method.

Runs	Time (min)	Heat transfer method (mm)	Direct method (mm)
1	43	0.494	0.453
2	13	0.486	0.440
3	33	0.547	0.419
4	5	0.474	0.404
5	45	0.550	0.608

increased very rapidly during the first few minutes. The fast deposition in the later runs is due to the already formed nucleation sites on the tube wall during the previous runs. The test results by heat transfer method were in good agreement with the data obtained from the direct method that consists into weighing the removed deposits from the testing tube after being drained (Table 3).

Critical temperature difference for deposit formation was introduced as variables to characterize the deposit formation tendency of the system. Once the deposition at the flowing solution and tube wall interface is formed, it behaves as a thermal insulation of the system and the temperature at the interface of the flowing solution and the deposited tube wall increases. There exists a critical temperature difference under which the formation of the deposit proceeds far slower than above this critical limit. The temperature rise T caused by the deposition formation as function of time t can be approximately by the Nyvlt equation (Nyvlt 1997):

$$logT = loga + b \cdot logt \quad [8]$$

The coefficient b can be obtained from the slope of the logarithm plot of solution temperature against time. The value of b significantly depends on the thermal gradient between the hot solution and the cooling water and this dependence can be approximately be a straight line, as shown in Figure 6. Extrapolation of the plot for $b \rightarrow 0$ enables a more exact evaluation of the critical

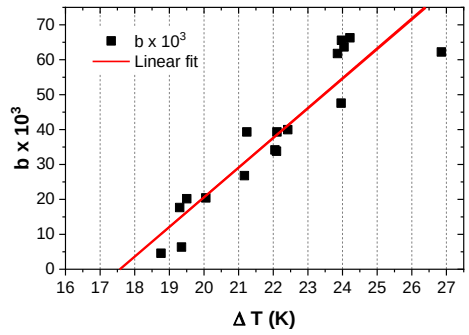

Figure 6: Critical temperature difference as a function of parameter b.

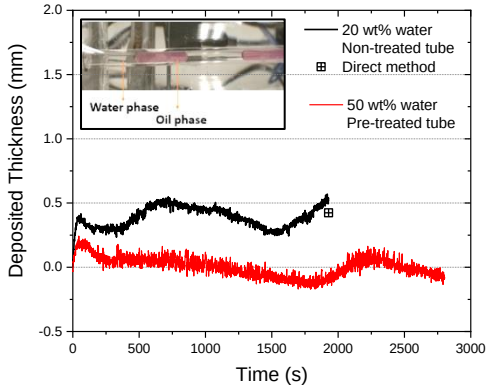

Figure 7: Measurement of deposited wax thickness of water/hydrocarbon mixture in the pre-treated and non-treated tubes. The inset shows the photo of water/ hydrocarbon mixture flow in pre-treated tube.

temperature difference. The obtained critical temperature difference is 17.6 K in this study, based on which the calculated saturated wax is 0.64. This analysis further verifies the measurement results based on the heat transfer method. The evaluation of pressure drop method on monitoring deposition process is ongoing.

The above discussed static study showed that the scaling tendency highly depends on the surface properties. As a verification in the dynamic test, the glass test tube was pre-treated by inserting in a 0.1N NaOH solution at 60 ^{o}C for 10 min. Depositions were then measured using a mixed water/hydrocarbon liquid flowing through the capillary as described above. In contrary to non-treated glass surfaces, no observable deposition formed in the pre-treated tube, as shown in Figure 7. This is because the NaOH etched glass is more hydrophilic. A water film formed on the tube surface, which prevents the direct contact of hydrocarbon solution with the tube wall and hence inhibits direct nucleation on the surface, under water/hydrocarbon flow. The premilitary test in dynamic condition proves the concept of mitigation deposit formation by the approach of modifying surface properties. The measurement of salt scale formation

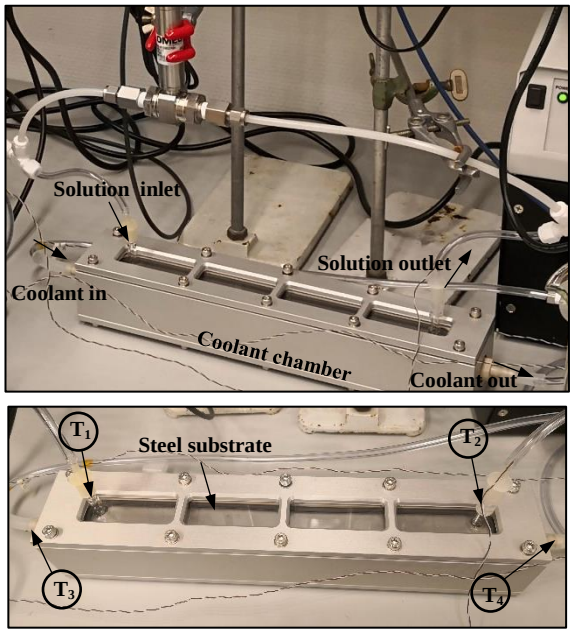

Figure 8: Test section of the flow loop to monitor deposition on flat substrate. The circled *T* symbols indicate the positions of thermocouples placed. They are used to measure temperature profiles of solution flow and coolant.

that is more practical in geothermal systems is under investigation in this developed flow loop system. The $CaCO_3$ scale will be formed under supersaturation conditions by employing binary stream flow of $CaCl_2$ solution and $NaHCO_3$ solution.

In addition to monitor deposition in a tube, a set-up capable of monitoring deposition dynamically on flat substrate has been designed, as shown in Figure 7. The set-up composed of two chambers, which are separated by a steel substrate or other interested substrate material. The substrate can be changed easily. The scaling solution flows through the upper chamber, and any deposition formed on the substrate can be monitored through the glass window in real time. The coolant flows through the lower chamber. The temperatures of the solution and coolant can be monitored. The flat substrate set-up is efficient for direct observation of scale deposition process on opaque substrate (e.g., steel) under flow condition, and is also suitable for surface characterization after deposition.

4. CONCLSIONS

In our previous study, a parameter that correlates the surface energy, the surface roughness, and the bulk modulus was developed to describe the scaling tendency of various systems under static scaling condition. In order to monitor and understand the mechanism of scaling kinetics under dynamic conditions, a flow loop system has been developed. The developed flow loop system provides a non-intrusive on-line method to monitor scale deposition inside a

tube or on a flat substrate under dynamic conditions and is capable to evaluate the effects of various parameters on encrustations formation. On one hand, the effective monitoring set-up is essential to serve the purpose of improving prediction of deposition formation by deepening understanding of the root cause and overall scaling kinetics. Moreover, it is crucial for the development of the scaling resistant coatings or materials to prevent deposition. The set-up can be potentially adapted to serve different study purpose, e.g. multi-deposition zones, binary stream flow, etc.

REFERENCES

Boersma, A., Vercauteren, F., Fischer, H. and Pizzocolo, F.: Scaling Assessment, Inhibition and Monitoring of Geothermal Wells, *Proceedings of the 43rd Workshop on Geothermal Reservoir Engineering*, Stanford, California, (2018), SGP-TR-213, 12-14.

Chaudhury, M.K., Finlay, J.A., Chung, J.Y., Callow, M.E. and Callow, J.A., The influence of elastic modulus and thickness on the release of the soft-fouling green alga Ulva linza from poly(dimethylsiloxane) model networks, *Biofouling*, (2005), 41-48.

Chen, X. T., Butler, T., Volk, M., & Brill, J. P.: Techniques for Measuring Wax Thickness During Single and Multiphase Flow. *SPE Annual Technical Conference and Exhibition*, San Antonio, Taxas, (1997), SPE-38773.

Chen, T., Wang, Q. and Chang, F.: $CaCO_3$ Scale Risk Assessment- Thermodynamic vs. Kinetics, *Corrosion 2016*, Vancouver, Canada, (2016). NACE-7263.

Cordoba, A.J., Schall, C.A.: Application of a heat transfer method to determine wax deposition in a hydrocarbon binary mixture, *Fuel*, (2001), 1285-1291.

Good, R.J., Chaudhury, M.K., and Yeung, C. A new approach for determining roughness by means of contact angles in solids, *Mittal. Festchrijft*, (1998), 181-197.

Kazmlerczak, T. F., Tomson, M. B. and Nancollas, G. H.: Crystal growth of calcium carbonate. A controlled compositions kinetics study, *Phys. Chem*, (1982), 86: 103–107.

Kendall, K.: The adhesion and surface energy of elastic solids. *J Phys D: Appl Phys 4*, (1971), 1186 – 1195.

Mavredaki, E., Neville, A.: Prediction and Evaluation of Calcium Carbonate Deposition at Surfaces, *SPE International Oilfield Scale Conference and Exhibition*, Aberdeen, Scotland (2014), SPE-169796-MS.

Nancollas, G.H. and Reddy, M. M.: The crystallization of calcium carbonate II. Calcite growth mechanism, *Journal of Colloid and Interface Science*, (1971), 37: 824–830.

Nyvlt, J. and Veverka, F.: Scale formation on cooling surfaces in crystallizers, *Cryst. Rea. Technol.*, (1997), 32: 773–781.

Van Krevelen, D.W., Properties of polymers, *Elsevier*, Amsterdam, (1997), p239.

Wang, Q., Liang, F., Al-Nasser, W., Al-Dawood, F., Al-Shafai, T., Al-Adairy, H., Shen, S. and Al-Ajwad, H.: Laboratory study on efficiency of three cacium carbonate scale inhibitors in the presence of EOR chemcals, *Petroleum*, (2018), 375-384.

Zhang, W., Hu, Y., Xi, L., Zhang, Y., Gu, H. and Zhang, T.: Preparation of Calcium Carbonate Superfine Powder by Calcium Carbide Residue, *Energy Proceedings*, (2012), 1635-1640.